

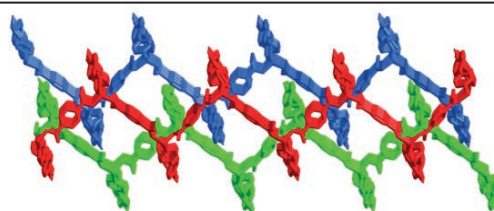
Luminescent 2D→3D porous zinc complex based on bis[4-(pyridin-4-yl)phenyl]amine and benzene-*p*-dicarboxylic acid

 Ming-Dao Zhang,^{*a,b} Yu Qiu,^a Ming-Xia Song,^a Shuo Ren,^a Cheng-Yan Huang^{*c} and Min-Dong Chen^a
^a Department of Chemistry, Jiangsu Key Laboratory of Atmospheric Environment Monitoring and Pollution Control, Jiangsu Collaborative Innovation Center of Atmospheric Environment, School of Environmental Science and Engineering, Nanjing University of Information Science & Technology, Nanjing 210044, Jiangsu, P. R. China. E-mail: matchlessjimmy@163.com
^b State Key Laboratory of Coordination Chemistry, Nanjing University, Nanjing 210093, P. R. China

^c School of Chemistry & Life Science, Nanjing University Jinling College, Nanjing 210089, Jiangsu, P. R. China. E-mail: inner-roy@163.com

DOI: 10.1016/j.mencom.2016.09.017

The luminescent coordination polymer $\{[\text{Zn}_2(\text{BPPA})_2(\text{bdc})_2](\text{H}_2\text{O})(\text{DMF})\}_n$ with a 2D→3D interpenetrating structure was constructed from Zn^{2+} ions, bis[4-(pyridin-4-yl)phenyl]amine (BPPA), and benzene-*p*-dicarboxylic acid (H_2bdc).



Recently, functional metal-organic frameworks (MOFs) have become a fast growing field of research due to their intriguing aesthetic structures^{1–3} and potential applications in photochemistry, molecular magnetism, gas adsorption, molecular separation, and heterogeneous catalysis.^{4–8}

Plenty of mixed-ligand coordination polymers have been reported, many of which include N-containing ligands introduced into metal–polycarboxylate systems. The combination of different ligands may result in greater tunability of structural frameworks compared to that with single ligands.

Among N-containing organic ligands, pyridyl ligands are often selected as multifunctional organic linkers because of their excellent coordination ability to meet the requirement of coordination geometries of metal ions.^{9–11} The semi-rigid ligand may provide a possibility for the construction of a steady large pore space framework.^{12–14}

The bis[4-(pyridin-4-yl)phenyl]amine (BPPA) ligand has been investigated intensely in the field of functional coordination polymers.¹⁵ A few complexes, featuring aesthetic structures or potential applications, have been constructed from BPPA. For instance, $\{[\text{Zn}_2(\text{BPPA})_2(\text{bdc})_2](\text{H}_2\text{O})_6\}_n$ (H_2bdc is benzene-*p*-dicarboxylic acid) represents a fourfold interpenetrated 3D network with sra topology; $\{[\text{Cd}_3(\text{BPPA})(\text{bdc})_2(\text{DMF})_2](\text{DMF})(\text{H}_2\text{O})_3\}_n$ is the first twofold interpenetrated sxa topology, which was previously reported only as non-interpenetrated.¹⁶

We tried to construct novel architectures when exploring the assembly of BPPA, carboxylic acids, and transition metal ions based on previous studies on BPPA. As a result, the new porous zinc complex $\{[\text{Zn}_2(\text{BPPA})_2(\text{bdc})_2](\text{H}_2\text{O})(\text{DMF})\}_n$ **1** was synthesized under solvothermal conditions based on H_2bdc and BPPA.[†]

The crystal structure determination has revealed that complex **1** crystallizes in monoclinic crystal system *C2/c*. The asymmetric unit of **1** contains two Zn^{2+} ions, two BPPA molecules, two bdc^{2-} anions, one lattice water molecule, and one DMF molecule. The valence states of Zn atoms in **1** were confirmed using the PLATON program.¹⁷ As shown in Figure 1,[‡] each Zn atom coordinates to

two oxygen atoms from two distinct bdc^{2-} anions and two nitrogen atoms from two BPPA molecules. The adjacent $\text{Zn}(1)\cdots\text{Zn}(2)$ distance is 10.94 Å. The Zn–O lengths are in a range of 1.94(14)–

[†] Reagents and solvents employed were commercially available and used as received. The BPPA ligand was synthesized according to the Suzuki aryl-coupling reaction.

*Synthesis of $\{[\text{Zn}_2(\text{BPPA})_2(\text{bdc})_2](\text{H}_2\text{O})(\text{DMF})\}_n$ **1**.* A mixture of $\text{Zn}(\text{NO}_3)_2 \cdot 6\text{H}_2\text{O}$ (29.7 mg, 0.1 mmol), bis[4-(pyridin-4-yl)phenyl]amine (BPPA) (32.3 mg, 0.1 mmol) and benzene-*p*-dicarboxylic acid (H_2bdc) (16.6 mg, 0.1 mmol) was dissolved in 15 ml of $\text{DMF}/\text{H}_2\text{O}$ (1:1). The final mixture was placed in a Parr Teflon-lined stainless steel vessel (25 ml) under autogenous pressure and heated at 95 °C for 3 days. Crystals of **1** were collected in 57% yield (based on BPPA ligand). IR (KBr, ν/cm^{-1}): 3463 (m), 3255 (m), 1669 (s), 1590 (s), 1531 (s), 1489 (s), 1435 (m), 1349 (s), 1323 (s), 1295 (s), 1227 (s), 1188 (m), 1075 (m), 1041 (s), 1018 (m), 818 (s), 748 (s). Found (%): C, 63.28; H, 4.34; N, 8.13. Calc. for $\text{C}_{63}\text{H}_{51}\text{N}_7\text{O}_{10}\text{Zn}_2$ (%): C, 63.22; H, 4.30; N, 8.19.

[‡] *Crystallographic data for **1*** ($\text{C}_{63}\text{H}_{51}\text{N}_7\text{O}_{10}\text{Zn}_2$, $M = 1196.85$). Monoclinic, space group *C2/c*, at 293 K: $a = 27.9964(19)$, $b = 18.1525(12)$, and $c = 23.0311(16)$ Å, $\beta = 102.1860(10)^\circ$, $V = 11440.8(13)$ Å³, $Z = 8$, $d_{\text{calc}} = 1.390$ g cm⁻³, $\mu(\text{MoK}\alpha) = 0.905$ mm⁻¹, $F(000) = 4944$. 31638 reflections were measured and 10073 independent reflections ($R_{\text{int}} = 0.0295$) were used in further refinement. The refinement converged to $wR_2 = 0.1155$ and GOF = 1.060 for all independent reflections [$R_1 = 0.0406$ was calculated against F for 7922 observed reflections with $I > 2\sigma(I)$]. X-ray crystallographic data of the complex were collected on a Bruker Apex Smart CCD diffractometer with graphite-monochromated MoK α radiation ($\lambda = 0.71073$ Å). The structure was solved by direct methods, and the non-hydrogen atoms were located from the trial structures and then refined anisotropically with SHELXTL using full-matrix least-squares procedures based on F^2 values.¹⁸ Hydrogen atoms positions were fixed geometrically at calculated distances and allowed to ride on the parent atoms. A semiempirical absorption correction was applied using SADABS.¹⁸ The topological analysis and some diagrams were produced using the TOPOS program.¹⁹

CCDC 1443016 contains the supplementary crystallographic data for this paper. These data can be obtained free of charge from The Cambridge Crystallographic Data Centre via <http://www.ccdc.cam.ac.uk>.

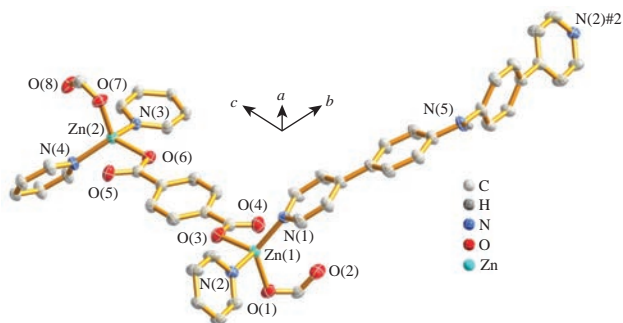


Figure 1 Coordination environment of complex **1**. The hydrogen atoms are omitted for clarity. Symmetry codes: #1 = $1.5 - x, 1.5 - y, -z$; #2 = $x, 1 + y, z$. Selected bond lengths (Å): O(1)–Zn(1) 1.9643(15), O(3)–Zn(1) 1.9763(17), O(6)–Zn(2) 1.9724(16), O(7)–Zn(2) 1.9372(14), N(1)–Zn(1) 2.0311(16), N(2)–Zn(1) 2.0709(17), N(3)–Zn(2) 2.0404(16), N(4)–Zn(2) 2.0239(16); selected bond angles (°): O(1)–Zn(1)–O(3) 106.09(7), O(1)–Zn(1)–N(1) 125.89(7), O(3)–Zn(1)–N(1) 115.43(7), O(1)–Zn(1)–N(2) 97.27(7), O(3)–Zn(1)–N(2) 101.59(7), N(1)–Zn(1)–N(2) 106.27(7), O(7)–Zn(2)–O(6) 105.74(7), O(7)–Zn(2)–N(4) 110.50(7), O(6)–Zn(2)–N(4) 121.42(7), O(7)–Zn(2)–N(3) 111.73(7), O(6)–Zn(2)–N(3) 99.12(7), N(4)–Zn(2)–N(3) 107.81(7).

1.98(17) Å, and the Zn–N lengths are 2.02(16)–2.07(17) Å. The dihedral angles between pyridyl and adjacent phenyl rings in the BPPA molecule and between phenyl rings are 9.5 and 58.3°, respectively.

For each bdc^{2-} anion in a unit of **1**, two carboxylate groups coordinated to Zn atoms in monodentate mode, forming a kind of 1D chains. Meanwhile, another kind of 1D chain is composed by BPPA molecules and Zn atoms. The O(1)–Zn(1)–O(3), O(6)–Zn(2)–O(7), N(1)–Zn(1)–N(2), and N(3)–Zn(2)–N(4) angles are 106.09, 105.74, 106.27, and 107.81°, respectively. These two kinds of 1D chains further form a 2D network by sharing the Zn^{2+} ions [Figure 2(a)]. Complex **1** contains a small solvent-accessible void space of 18.4% of the total crystal volume calculated by the PLATON program.¹⁷ Recently, attention was focused on 2D coordination networks containing cavities or channels because of their function in finely tuning the shape and size of the cavities. Figure 2(a) shows that each window of the ladder-like chains in **1** includes four Zn^{2+} ions, two BPPA molecules, and two bdc^{2-} anions. The windows in each network are large enough to accommodate two other adjacent networks [Figure 2(c)], which exhibit interpenetrating networks.

A better insight into this intricate network can be accessed by a topological method.¹⁹ The Zn atoms can be regarded as four-connected nodes, and BPPA ligands and bdc^{2-} anions can be

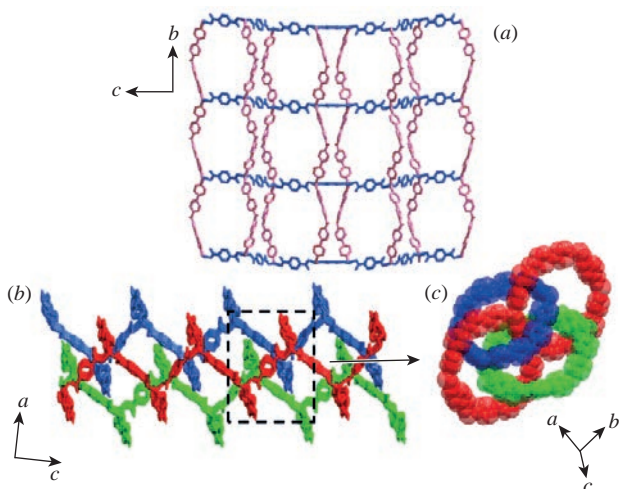


Figure 2 (a) Ladder-like single 2D framework of **1**; (b) 2D layers accumulated in a single direction, confirming the interpenetrating architecture in **1**; (c) schematic representation of the interpenetrating architecture of compound **1**.

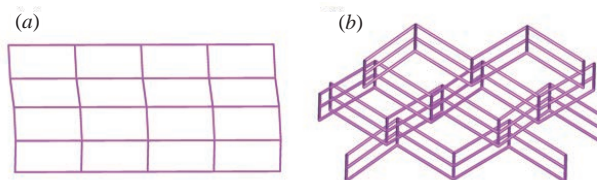


Figure 3 (a) Perspective view of the single 2D network of **1** (BPPA ligand and bdc^{2-} anions were simplified into linkers); (b) packing drawing of a simplified structure of **1**.

regarded as linkers. The linkers of one layer pass through the cavity of the others; therefore, 2D interpenetrating networks are formed [Figure 3(a)]. The Schläfli symbol for this binodal net is $\{4^4.6^2\}$, and the topological type is sql. Figure 3(b) shows the simplified structure of **1**; the adjacent sql networks in **1** do not entangle with each other.

In addition, the UV-visible absorption spectra of complex **1** in a crystalline state were measured at room temperature (BPPA and H_2bdc in solid state) [Figure 4(a)]. BPPA and H_2bdc show intense absorption peaks at 200–450 and 280–330 nm, respectively, which can be ascribed to the π – π^* transitions of ligands. Energy bands of complex **1** from 210–500 nm are attributed to the internal π – π^* transitions of the ligands.

Luminescent complexes are of great interest due to various applications in chemical sensors, photochemistry, and light-emitting diodes (LEDs). Figure 4(b) indicates that both the free BPPA ligand and complex **1** exhibit intense emissions between 440 and 540 nm. The emission peaks of compound **1** ($\lambda_{\text{max}} = 481$ nm upon excitation at 350 nm) and the BPPA ligand ($\lambda_{\text{max}} = 468$ nm upon excitation at 350 nm) have similar profiles and almost the same location, indicating that the emission of **1** can be mostly attributed to the charge transfer of internal BPPA ligand. The emission peaks of **1** are slightly red-shifted compared to BPPA, probably, due to weaker ligand-to-metal charge transfer (LMCT) in **1**.

In conclusion, the new fascinating 2D→3D zinc coordination polymer $\{[\text{Zn}_2(\text{BPPA})_2(\text{bdc})_2](\text{H}_2\text{O})(\text{DMF})\}_n$ **1** containing a solvent-

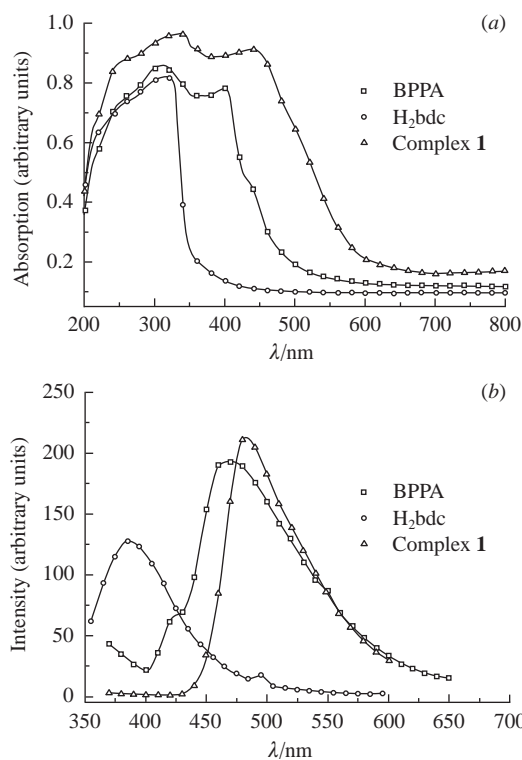


Figure 4 (a) UV-visible absorption spectra of ligands and **1**; (b) emission spectra of a free BPPA ligand, H_2bdc and **1** (solid state) at room temperature.

accessible void space of 18.4% was prepared under solvothermal conditions based on H₂bdc and BPPA. The crystal structure of **1** was characterized, and the photophysical properties of **1** were investigated and discussed in detail.

This work was supported by the Natural Science Foundation of China (grant nos. 21401107, 11305091, and 21577065), the Natural Science Foundation of Jiangsu, China (grant nos. BK20140986 and BK20131429), the International ST Cooperation Program of China (grant no. 2014DFA90780), Natural Science Foundation of the Jiangsu Higher Education Institutions of China (grant no. 14KJB150013), as well as by a project funded by the Priority Academic Program Development of Jiangsu Higher Education Institutions (PAPD) and the Jiangsu Engineering Technology Research Center of Environmental Cleaning Materials.

References

- J.-S. Hu, X. M. Zhang, H.-L. Xing, J. He and J.-J. Shi, *Mendeleev Commun.*, 2013, **23**, 231.
- A. K. Eckert, O. N. Trukhina, M. S. Rodríguez-Morgade, E. A. Danilova, M. K. Islyaikin and T. Torres, *Mendeleev Commun.*, 2010, **20**, 192.
- V. M. Kovrugin, V. V. Gurzhiy, S. V. Krivovichev, I. G. Tananaev and B. F. Myasoedov, *Mendeleev Commun.*, 2012, **22**, 11.
- L. L. Johnston, J. H. Nettleman, M. A. Braverman, L. K. Sposato, R. M. Supkowski and R. L. LaDuca, *Polyhedron*, 2010, **29**, 303.
- B. Xu, X. Lin, Z. He, Z. Lin and R. Cao, *Chem. Commun.*, 2011, **47**, 3766.
- L. J. Murray, M. Dincă and J. R. Long, *Chem. Soc. Rev.*, 2009, **38**, 1294.
- L. Qin, J.-S. Hu, M.-D. Zhang, Z.-J. Guo and H.-G. Zheng, *Chem. Commun.*, 2012, **48**, 10757.
- A. L. Nuzhdin and G. A. Bukhtiyarova, *Mendeleev Commun.*, 2015, **25**, 153.
- J.-S. Hu, C.-H. Zhou, Y.-M. Wang, K.-P. Xu and Y.-W. Li, *Mendeleev Commun.*, 2015, **25**, 211.
- M.-D. Zhang, Y. Jiao, J. Li and M.-D. Chen, *Mendeleev Commun.*, 2015, **25**, 65.
- M. Hu, Z.-W. Wang, H. Zhao and S.-M. Fang, *Mendeleev Commun.*, 2015, **25**, 150.
- L. C. Rowsell and O. M. Yaghi, *Angew. Chem. Int. Ed.*, 2005, **44**, 4670.
- B. Chen, N. W. Ockwig, A. R. Millward, D. S. Contreras and O. M. Yaghi, *Angew. Chem. Int. Ed.*, 2005, **44**, 4745.
- T. K. Trung, P. Trens, N. Tanchoux, S. Bourrelly, P. L. Llewellyn, S. Loera-Serna, C. Serre, T. Loiseau, F. O. Fajula and G. Férey, *J. Am. Chem. Soc.*, 2008, **130**, 16926.
- M.-D. Zhang, Z. Wang, Y. Qiu, J.-M. He, X. Liu and C.-Z. Zhang, *Mendeleev Commun.*, 2015, **25**, 296.
- Z.-J. Wang, L. Qin, X. Zhang, J.-X. Chen and H.-G. Zheng, *Cryst. Growth Des.*, 2015, **15**, 1303.
- P. Van der Sluis and A. L. Spek, *Acta Crystallogr., Sect. A.*, 1990, **46**, 194.
- Bruker 2000, *SMART (Version 5.0)*, *SAINt-plus (Version 6)*, *SHELXTL (Version 6.1)* and *SADABS (Version 2.03)*, Bruker AXS Inc., Madison, WI.
- V. A. Blatov, *Struct. Chem.*, 2012, **23**, 955.
- M. D. Allendorf, C. A. Bauer, R. K. Bhakta and R. J. T. Houk, *Chem. Soc. Rev.*, 2009, **38**, 1330.
- S.-L. Zheng, J.-H. Yang, X.-L. Yu, X.-M. Chen and W.-T. Wong, *Inorg. Chem.*, 2004, **43**, 830.

Received: 12th January 2016; Com. 16/4815